

Evaporation of a Sessile Microdroplet on a Heated Hydrophobic Substrate

Nagesh D. Patil and Rajneesh Bhardwaj*

Department of Mechanical Engineering,
Indian Institute of Technology Bombay, Mumbai, 400076 India

*Corresponding author: rajneesh.bhardwaj@iitb.ac.in

ABSTRACT

We investigated evaporation of sessile water microdroplets on heated hydrophobic glass substrate. An in-house, experimentally validated finite-element numerical model was employed to simulate internal fluid flow and heat transfer during the evaporation. We also validated the non-uniform evaporative flux for water droplets having different initial wetting angles with theoretical results from literature. During evaporation, the fluid flow is radially outward due to the largest evaporative flux near the wetting line. The isotherms are almost horizontal which indicates that the conduction between the droplet and substrate dominates over internal convection during the evaporation. The evolution of wetted radius and wetting angle indicates a two-stage evaporation process: during the first stage of the evaporation, wetted radius remains constant and wetting angle decreases with time; while in the second stage, wetting angle remains constant and wetted radius decreases with time. The droplet volume shows a linear decrease in the first stage and an exponential decrease in the second stage. We compared the time-varying droplet volume, height, wetted radius and wetting angle with respective published measurements. The comparisons are good and verify our numerical model.

1. INTRODUCTION

The evaporation of a droplet on a hydrophobic substrate has applications in spray evaporative cooling [1, 2], ink-jet printing [3] and self-cleaning technologies [4, 5]. The physics involved during the evaporation is complex interplay of several transport phenomena. The droplet evaporation occurs by liquid-vapor diffusion in quiet atmosphere and is influenced by relative humidity of the ambient. The evaporative flux on the free surface is non-uniform and the largest evaporation near the contact line generates evaporative-driven radially outward and transient internal flow [6, 7]. The heat transfer occurs by internal convection in the droplet and conduction in the heated substrate. Laplace forces on the liquid-gas boundary are larger due to small length scales ($O(\mu\text{m})$) and receding of the contact line governed by Young-Dupré law [8] may occur during the evaporation. In general, evaporation occurs in two stages [9, 10]: first, constant contact radius (CCR) stage, in which the droplet wetted radius pins to the substrate and wetting angle decreases with time; second, constant contact angle (CCA) stage, in which the wetting angle remains constant and wetted radius decreases with time (Figure 1a).

Studies of the sessile droplet evaporation on hydrophilic, hydrophobic and superhydrophobic substrates were recently reviewed by Cazabat and Guéna [11]. Extending Popov's droplet evaporation model [12] to hydrophobic and superhydrophobic substrates, Gelderblom et al. [13] proved that the evolution of the droplet volume and wetting angle can be collapsed to one numerical curve for all droplet volumes and wetting angles. The CCA and CCR evaporation stages on hydrophobic/superhydrophobic substrates were characterized in similar studies [14-17]. Recent studies have also focused on the effect of wetting transition from Cassie to Wenzel state on microstructured substrates [18, 19]. However, very few studies were reported on evaporation of microdroplets on heated

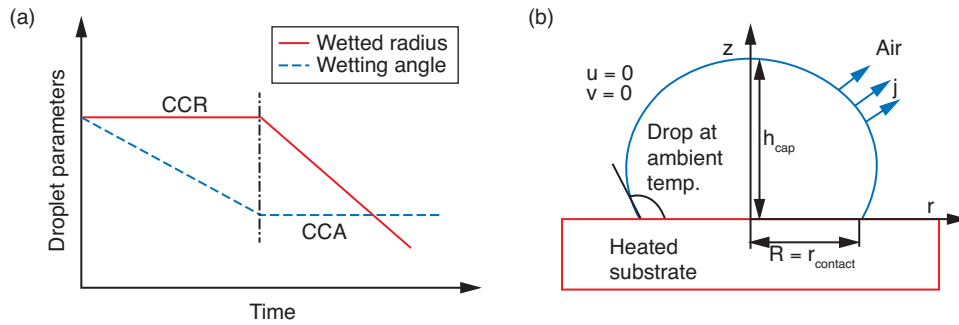


Figure 1. a) Schematic of two evaporation stages, b) A sessile spherical cap droplet on a hydrophobic substrate

hydrophobic substrates. For instance, Putnam et al. [20] studied contact line dynamics of water droplets at different substrate temperatures. The measurements of the internal flow and temperature fields are not trivial and the numerical data coupled with measurements in the literature will help to establish flow and thermal fields with evaporation dynamics. In this context, the goal of the present work is to employ an in-house, experimentally validated solver [21] for the droplet evaporation on hydrophobic substrates and compare the simulated results with the published measurements in order to understand the evaporation dynamics coupled with internal flow and thermal fields.

2. NUMERICAL MODEL

We employed an in-house, experimentally-validated finite-element numerical model [21, 22] for simulating the droplet evaporation on a hydrophobic substrate. The model solves the Navier-Stokes, energy and mass transport equations in axisymmetric, cylindrical, Lagrangian coordinates. The evaporative flux at the droplet-air free surface is calculated by solving diffusion equation for liquid vapour concentration outside the droplet. The details of the algorithm can be found in Ref [21]. The code was validated extensively for the evaporation of water droplets [23], isopropanol droplets [22] and colloidal droplets [21, 24] on hydrophilic substrates. In the present study, the model is extended to investigate droplet evaporation on a heated hydrophobic substrate, as shown in Figure 1b. The variation of viscosity with temperature is taken into account while the Marangoni stresses due to surface tension gradient are neglected.

Validation of Evaporative flux on Hydrophobic Substrate

The non-uniform evaporative flux in the present model was validated for hydrophilic substrates in earlier studies [21-23]. In present work, we validated evaporative flux (j) for hydrophobic substrates against results given in Ref. [25] with initial wetting angles $\theta = 90^\circ$, 120° and 135° for different volumes of the droplet. As plotted in Figure 2, the comparisons are in good agreement and validate our evaporation model. The evaporative flux is almost constant for wetting angle 90° . For $\theta > 90^\circ$, the evaporative flux decreases from the droplet centre ($r = 0$) and to the edge ($r = r_{\text{contact}}$), and further decaying to zero at the wetting line (Figure 2, right). The evaporative flux is zero due to wedge region, which restricts the liquid-vapor diffusion (Figure 2, left).

3. RESULTS AND DISCUSSION

We compare simulated evaporation of a picoliter water droplet on a heated hydrophobic glass substrate coated with aluminum thin-film, against measurements of Putnam et al. [20]. The parameters of the cases selected for the comparisons are given in Table 1. Figure 3 compares the simulation results for the evaporation of a 90 pL water droplet on the heated substrate at 100°C with measurements. We plotted the time-variation of droplet volume, height, wetted radius and wetting angle, normalized with

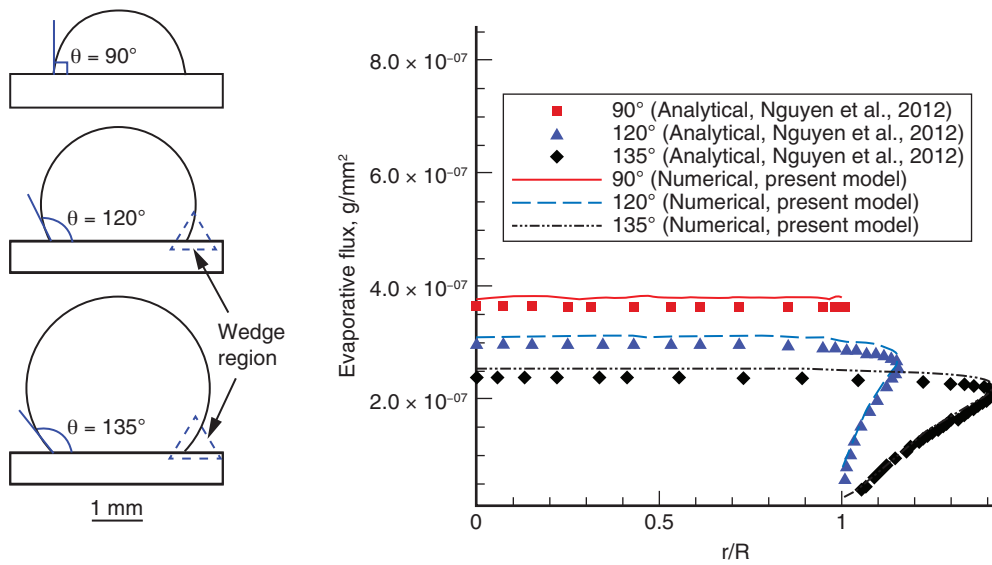


Figure 2. Variation of evaporative flux for different wetting angles with droplet radial position along wetting line (right), droplet shape with different initial wetting angles (left). The wetted radius of the droplet, diffusion coefficient of water vapour, vapour concentration at droplet-air interface, the droplet temperature and relative humidity are 1 mm, 26.1 mm²/s, 2.32×10⁻⁸ g/mm³, 25°C and 40%, respectively.

Table 1. Details of experimental values used by Putnam et al. [20]. The droplet is at ambient temperature (25°C) condition with 30% relative humidity of air.

Case No.	T_{sub} (°C)	Volume (pL)	$r_{contact}$ (µm)	h_{cap} (µm)	θ (°)	t_{evp} (ms)	t_{rec} (ms)
1	100	90	34.6	35.2	91	58.5	32
2	118.5	977.5	64.2	91.3	111	200	100

respect to the respective initial values ($t = 0$ ms) in Figure 3. During the first stage of evaporation (CCR) ($t = 0$ to 34 ms), the wetting line is pinned which means wetted radius remains constant (blue, dashed line in Figure 3) and the internal flow is radially outward, as shown by streamlines in insets of Figure 3, (right frames). The outward flow is due to the fact that liquid evaporated from the edge must be replenished by the inner liquid. In this stage, the wetting angle decreases with time (black, dashed dotted line in Figure 3). During the second stage of evaporation (CCA), ($t = 34$ to 64 ms), the wetting line starts receding. The wetting angle remains constant with time and wetted radius decreases non-linearly with time. The receding angle in the model was taken as 50° from the experiment. The time-variation of the droplet volume shows linear decrease for the first stage (CCR) while droplet exhibits exponential decrease in the second stage (CCA). The receding occurs at 32 ms as compared to simulated value of 34 ms, with a relative error of around 6%. The receding occurs at around 50% of the total drying time. The numerical results of the evaporating microdroplet shapes with streamlines (right half) and isotherms (left half) at different time instances ($t = 0, 19, 34.6$ and 55.4 ms) are shown in the insets of Figure 3. The horizontal isotherms indicate that the conduction heat transfer from the substrate dominates over the convective heat transfer inside the droplet. The isotherms meet the vertical axis orthogonally because of axisymmetry boundary condition. The temperature inside the droplet varies from 70°C at the top to 85°C at the wetting line. Figure 4 compares numerical results with

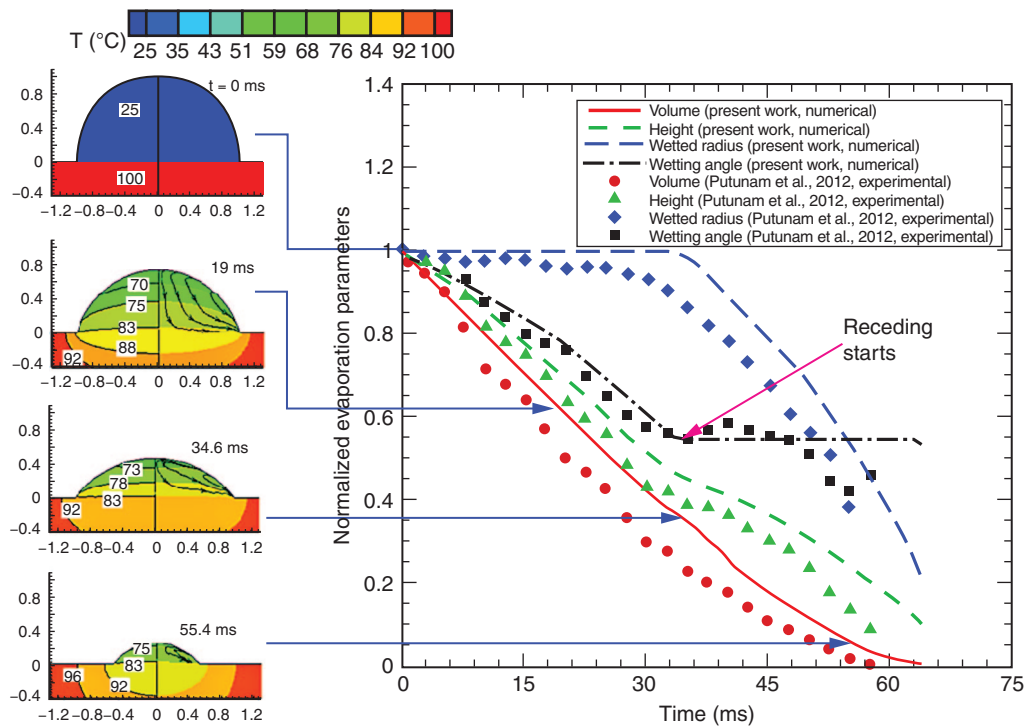


Figure 3. Comparison between present simulation and experiment of Putnam et al. [20] for the evaporation of 90 pL water droplet. The initial substrate temperature, droplet temperature and wetting angle are 100°C, 25°C and 91°, respectively

measurements of Putnam et al. [20] for case 2 (Table 1) for initial droplet volume of 977.5 pL. The wetted radius, wetting angle, receding angle and the substrate temperature are 64.2 μm , 111°, 75° and 118.5°C respectively. We note the CCR and CCA stages for times 0-114 ms and 114-246 ms in this case, respectively, similar to those described in case 1. The calculated time of the incipience of receding is 114 ms as compared to measured time of 100 ms, with a relative error of 14%. The recorded time taken for receding is around 50% of the drying time, similar to that in case 1. The simulated drying time of the droplet (250 ms) is around 25% larger than the measured value (200 ms). As seen in case 1, the conduction heat transfer dominates over the internal convection as demonstrated by horizontal isotherms in Figure 4. Overall, the comparison of numerical and experimental results demonstrate that the present in-house finite element numerical model [21, 22] is valid for evaporation of a droplet on a heated hydrophobic substrate and the numerical results render useful data on flow and thermal fields.

4. CONCLUSIONS

The evaporation of a microdroplet on a heated hydrophobic substrate was investigated numerically and simulations were compared with published experimental results. An in-house, experimentally validated finite-element numerical model was employed and validated for non-uniform evaporative flux on hydrophobic substrate in the present study. The internal fluid flow is radially outward due to the highest evaporative flux near the wetting line. The conduction heat transfer inside the droplet dominates over convection. We note two stages of evaporation: constant contact radius (CCR) followed by constant contact angle (CCA). In first stage of the evaporation, the droplet volume decreases linear while in later stage as droplet starts receding, the volume decreases exponentially. The comparisons of the time-varying droplet volume, height, wetted radius, and wetting angle are good and verify the numerical model. The numerical data helps to gain insights in the internal flow and thermal fields.

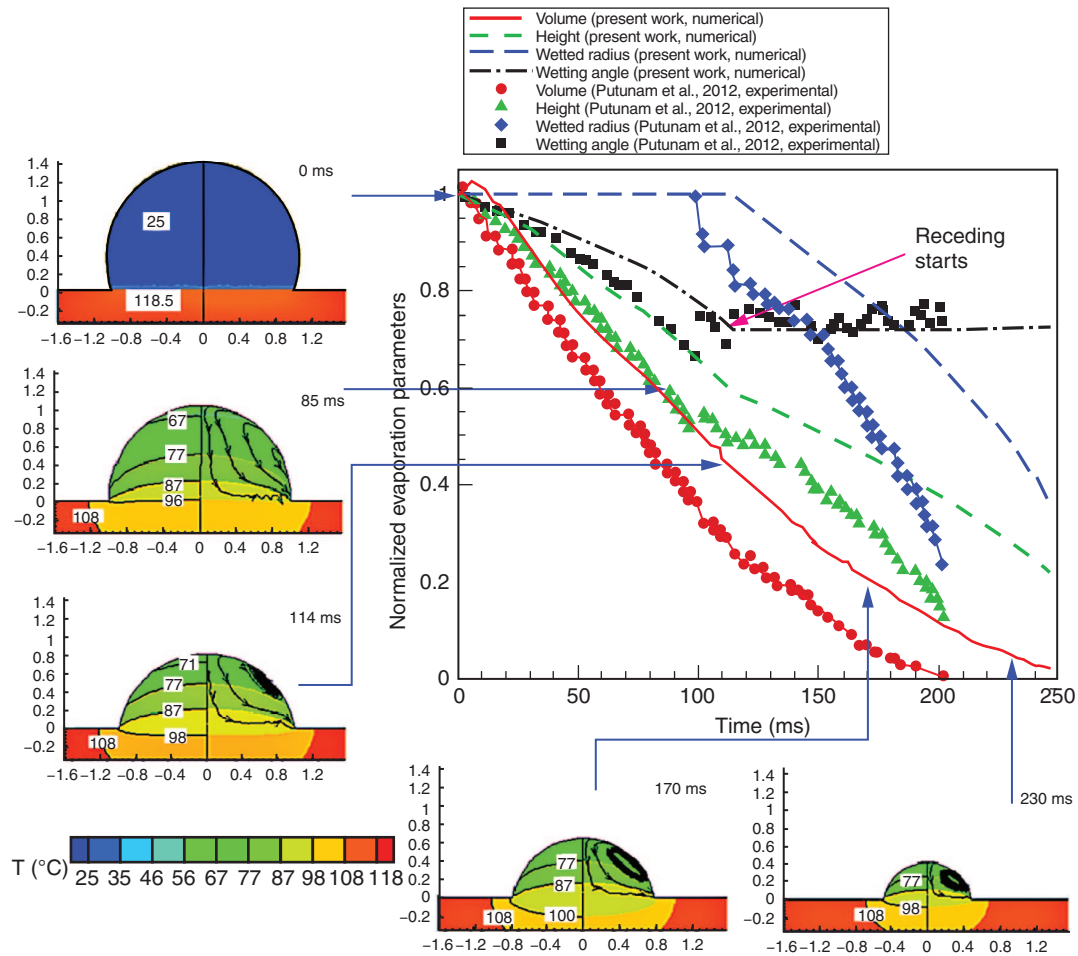


Figure 4. Comparison between present simulation and experiment of Putnam et al. [20] for the evaporation of 977.5 pL water droplet. The initial substrate temperature, droplet temperature and wetting angle are 118.5°C, 25°C and 111°, respectively

ACKNOWLEDGEMENTS

We gratefully acknowledge financial support from Department of Science and Technology (DST), New Delhi through fast track scheme for young scientists. The work was also partially supported by internal grant from Industrial Research and Consultancy Centre (IRCC), IIT Bombay. N.D.P was supported by Ph.D. student fellowship awarded by IRCC, IIT Bombay.

REFERENCES

- [1] Y. Joshi, and S. Garimella, *Thermal challenges in the next generation electronic systems*, Microelectronics, 2003, 34, 169.
- [2] N.D. Patil, P.K. Das, S. Bhattacharyya, and S.K. Sahu, *An experimental assement of cooling of a 54-rod bundle by in-bundle injection*, Nuclear Engineering and Design, 2012, 250, 500–511.
- [3] J.A. Lim, W.H. Lee, H.S. Lee, J.H. Lee, Y.D. Park, and K. Cho, *Selforganization of ink-jet-printed triisopropylsilylethynyl pentacene via evaporationinduced flows in a drying droplet*. Advanced functional materials, 2008, 18, 229–234.
- [4] R. Blossey, *Self-Cleaning Surfaces-Virtual Realities*, Nature Materials, 2003, 2, 301–306.

- [5] Y. Liu, J.H. Xin, and C.H. Choi, *Cotton Fabrics with Single-Faced Superhydrophobicity*, *Langmuir*, 2012, 28, 17426–17434.
- [6] R. D. Deegan, O. Bakajin, T.F. Dupont, G. Huber, S.R. Nagel, and T.A. Witten, *Capillary flow as the cause of ring stains from dried liquid drops*, *Nature*, 1997, 389, 827–829.
- [7] H. Hu, and R.G. Larson, *Evaporation of a sessile droplet on a substrate*, *J. Phys. Chem. B* 2002, 106, 1334–1344.
- [8] P.-G. De Gennes, F. Brochard-Wyart, and D. Quéré, *Capillarity and wetting phenomena: drops, bubbles, pearls, waves*, Springer, 2004.
- [9] R. G. Picknett, and R. Bexon, *The evaporation of sessile or pendant drops in still air*. *J. Colloid Interface Sci.*, 1977, 61(2), 336–350.
- [10] K.S. Birdi, and D.T. Vu, *Wettability and the evaporation rates of fluids from solid surface*, *J. Adhesion Sci. Technol.*, 1993. 7(6): p. 485–493.
- [11] A.-M. Cazabat, and G. Guéna, *Evaporation of macroscopic sessile droplets*, *Soft Matter*, 2010, 6(12), 2591–2612.
- [12] Y.O. Popov, *Evaporative deposition patterns: Spatial dimensions of the deposit*, *Phys. Rev. E*, 2005, 71, 0363131–03631317.
- [13] H. Gelderblom, A.G. Marin, H. Nair, A.v. Houselt, L. Lefferts, J.H. Snoeijer, and D. Lohse, *How water droplets evaporate on a superhydrophobic substrate*, *Phys. Rev. E*, 2011, 83, 0263061–0263065.
- [14] G. McHale, S. Aqil, N.J. Shirtcliffe, M.I. Newton, and H.Y. Erbil, *Analysis of droplet evaporation on a superhydrophobic surface*, *Langmuir*, 2005, 21, 11053–11060.
- [15] X. Zhang, S. Tan, N. Zhao, X. Guo, X. Zhang, Y. Zhang, and J. Xu, *Evaporation of sessile water droplets on superhydrophobic natural lotus and biomimetic polymer surfaces*, *ChemPhysChem*, 2006, 7(10), 2067–2070.
- [16] D.H. Shin, S.H. Lee, J.-Y. Jung, and J.Y. Yoo, *Evaporating characteristics of sessile droplet on hydrophobic and hydrophilic surfaces*, *Microelectronic Engineering*, 2009, 86(4), 1350–1353.
- [17] D.H. Shin, S.H. Lee, C.K. Choi, and S. Retterer, *The evaporation and wetting dynamics of sessile water droplets on submicron-scale patterned silicon hydrophobic surfaces*, *J. of Micromechanics and Microengineering*, 2010, 20(5), 055021.
- [18] X. Chen, R. Ma, J. Li, C. Hao, W. Guo, B.L. Luk, S.C. Li, S. Yao, and Z. Wang, *Evaporation of droplets on superhydrophobic surfaces: Surface roughness and small droplet size effects*, *Physical Review Letters*, 2012, 109(11), 116101.
- [19] W. Xu, R. Leeladhar, Y.T. Kang, and C.-H. Choi, *Evaporation kinetics of sessile water droplets on micropillared superhydrophobic surfaces*, *Langmuir*, 2013, 29(20), 6032–6041.
- [20] S.A. Putnam, A.M. Briones, L.W. Byrd, J.S. Ervin, M.S. Hanchak, A. White, and J.G. Jones, *Microdroplet evaporation on superheated surfaces*, *Int. J. of Heat and Mass Transfer*, 2012, 55, 5793–5807.
- [21] R. Bhardwaj, X. Fang, and D. Attinger, *Pattern formation during the evaporation of a colloidal nanoliter drop: A numerical and experimental study*, *New Journal of Physics*, 2009, 11, 075020.
- [22] R. Bhardwaj, J.P. Longtin, and D. Attinger, *Interfacial temperature measurements, high-speed visualization and finite-element simulations of droplet impact and evaporation on a solid surface*, *Int. J. of Heat and Mass Transfer*, 2010, 53, 3733–3744.
- [23] R. Bhardwaj, J.P. Longtin, and D. Attinger, *A numerical investigation on the influence of liquid properties and interfacial heat transfer during microdroplet deposition onto a glass substrate*, *Int. J. of Heat and Mass Transfer*, 2007, 50, 2912–2923.
- [24] R. Bhardwaj, X. Fang, P. Somasundaran, and D. Attinger, *Self-assembly of colloidal particles from evaporating droplets: Role of dlvo interactions and proposition of a phase diagram*, *Langmuir*, 2010, 26(11), 7833–7842.

- [25] T.A.H. Nguyen, A.V. Nguyen, M.A. Hampton, Z.P. Xu, L. Huang, and V. Rudolph, *Theoretical and experimental analysis of droplet evaporation on solid surfaces*, J. Chem. Engg. Sci., 2012, 69, 522–529.

¹ Joshi and Garimella (2002)

² Patil et al. (2012)

³ Lim et al. (2008)

⁴ Blossey (2003)

⁵ Liu et al. (2012)

⁶ Deegan et al. (1997)

⁷ Hu and Larson (2002)

⁸ De Gennes et al. (2004)

⁹ Picknett and Bexon (1978)

¹⁰ Birdi et al. (1993)

¹¹ Cazabat and Guéna (2010)

¹² Popov (2005)

¹³ Gelderblom et al. (2011)

¹⁴ McHale et al. (2005)

¹⁵ Zhang et al. (2006)

¹⁶ Shin et al. (2009)

¹⁷ Shin et al. (2010)

¹⁸ Chen et al. (2012)

¹⁹ Xu et al. (2013)

²⁰ Putnam et al. (2012)

²¹ Bhardwaj et al. (2009)

²² Bhardwaj et al. (2010)

²³ Bhardwaj et al. (2007)

²⁴ Bhardwaj et al. (2010)

²⁵ Nguyen et al. (2012)

